Title
Long-term in vivo electromechanical reshaping for auricular reconstruction in the New Zealand white rabbit model.

Journal
The Laryngoscope, 125(9)

ISSN
0023-852X

Authors
Badran, Karam W
Manuel, Cyrus T
Loy, Anthony Chin
et al.

Publication Date
2015-09-01

DOI
10.1002/lary.25237

HHS Public Access

Author manuscript

Laryngoscope. Author manuscript; available in PMC 2016 February 02.

Published in final edited form as:

Laryngoscope. 2015 September ; 125(9): 2058–2066. doi:10.1002/lary.25237.

Long-Term In Vivo Electromechanical Reshaping for Auricular Reconstruction in the New Zealand White Rabbit Model

Karam W. Badran, MD, **Cyrus T. Manuel, BSc**, **Anthony Chin Loy, MD**, **Christian Conderman, MD**, **Yuk Yee Yau, MD**, **Jennifer Lin, MD**, **Tjoson Tjoa, MD**, **Erica Su, BSc**, **Dmitriy Protsenko, PhD**, and **Brian J. F. Wong, MD, PhD**

Beckman Laser Institute (K.W.B., C.T.M., A.C.L., C.C., Y.Y.Y., J.L., T.T., E.S., D.P., B.J.F.W.), University of California–Irvine, Irvine, California; the Department of Head and Neck Surgery (K.W.B.), University of California–Los Angeles, Los Angeles, California; and the Department of Otolaryngology, Head and Neck Surgery (A.C.L., C.C., Y.Y.Y, J.L., T.T., B.J.F.W.), University of California–Irvine, Orange, California, U.S.A

Abstract

Objectives/Hypothesis—To demonstrate the dosimetry effect of electromechanical reshaping (EMR) on cartilage shape change, structural integrity, cellular viability, and remodeling of grafts in an in vivo long-term animal model.

Study Design—Animal study.

Methods—A subperichondrial cartilaginous defect was created within the base of the pinna of 31 New Zealand white rabbits. Autologous costal cartilage grafts were electromechanically reshaped to resemble the rabbit auricular base framework and mechanically secured into the pinna base defect. Forty-nine costal cartilage specimens (four control and 45 experimental) successfully underwent EMR using a paired set of voltage-time combinations and survived for 6 or 12 weeks. Shape change was measured, and specimens were analyzed using digital imaging, tissue histology, and confocal microscopy with LIVE-DEAD viability assays.

Results—Shape change was proportional to charge transfer in all experimental specimens ($P <$ .01) and increased with voltage. All experimental specimens contoured to the auricular base. Focal cartilage degeneration and fibrosis was observed where needle electrodes were inserted, ranging from 2.2 to 3.9 mm. The response to injury increased with increasing charge transfer and survival duration.

Conclusions—EMR results in appropriate shape change in cartilage grafts with chondrocyte injury highly localized. These studies suggest that elements of auricular reconstruction may be

Send correspondence to: Brian J. F. Wong, MD, Beckman Laser Institute, University of California–Irvine, 10002 Health Sciences Road, Irvine, California 92612. bjwong@uci.edu.

Level of Evidence: NA

This work was completed at the Beckman Laser Institute and Medical Clinic, University of California–Irvine, Irvine, California, U.S.A.

Brian J. F. Wong, MD, has had intellectual property licensed for the development of this technology. Dr. Wong has equity interest in Praxis BioSciences, which is commercializing this technology.

The authors have no other funding, financial relationships, or conflicts of interest to disclose.

feasible using EMR. Extended survival periods and further optimization of voltage-time pairs are necessary to evaluate the long-term effects and shape-change potential of EMR.

Keywords

Electromechanical reshaping; otoplasty; auricular reconstruction; microtia repair; animal model

INTRODUCTION

Current techniques for the reconstruction of the cartilaginous auricular framework have evolved from the contributions of Tanzer, Brent, Firmin, and Nagata.[1–4] Traditional microtia repair creates an auricular scaffold by carving the synchondrosis and by attaching curved sections of costal cartilage, which is then secured to the framework base using sutures. Cartilage innately resists deformation, and these internal forces must be balanced extrinsically by securing shape change using stainless steel wire or other nonabsorbable sutures. Carving techniques, though time honored and well established, are limited in that substantial tissue is discarded. The area occupied by the cartilage framework in a native ear is rather modest and less than 1,000 mm^2.[5] Therefore, if cartilage could be precisely cut into thin (1–2 mm) sections,[6] then it may be possible to construct a thinner, more pliable framework, using suture fixation as a means to assemble a scaffold and maintain curvature. This could be accomplished using only one rib segment.[7] Optimizing the creation of stable curvature and shape change in this approach to reconstruction has major clinical implications.

Electromechanical reshaping (EMR) is a novel technique that has been shown to permanently change the shape of cartilaginous tissue through in situ electrochemical (redox) reactions.[8,9] Low amplitude voltage is applied to needle electrodes in mechanically stressed regions of tissue. The electric field created within the tissue-electrode interface initiates redox reactions in the matrix that lead to the relaxation of internal stress with sustained shape change (Fig. 1).[10]

Alternative methods of reshaping cartilage, such as laser, have been extensively studied. Several studies demonstrate chondrocyte viability following laser irradiation in vivo, though simultaneous shape change within these parameters have yet to be identified.[11–13] Despite the presence of viable chondrocytes within a laser irradiated specimen, in vivo experimentation has demonstrated focal loss in structural integrity and changes in mechanical stability, manifesting as shape change.[14] By contrast, EMR does not produce significant temperature changes and has been demonstrated to cause shape change when applied in vivo.[9,10,15] Additionally, EMR can be performed with inexpensive needle electrodes and direct current power supplies (e.g., watch batteries).

Previously, EMR has been systematically studied in ex vivo costal cartilage to identify a set of voltage and time parameters that recreate the curvature of the auricular base in the New Zealand white rabbit.[9,10,15] To advance this technology toward clinical application, additional information on the behavior of cartilage grafts following EMR is necessary, in particular, how the tissue evolves after implantation in an animal with intact wound healing mechanisms. Therefore, in vivo assessment as a function of dosimetry and electrode

configuration is necessary. The present study aimed to investigate EMR dosimetry on long-term cartilage shape change and stability, structural integrity, cellular viability, and remodeling of costal grafts in an in vivo animal model."

MATERIALS AND METHODS

Thirty-one New Zealand white rabbits (Western Oregon Rabbit Company, Philomath, OR), weighing 3.9 to 4.1 kg, were used in the study. All protocols and experimental design settings were approved by the University of California, Irvine Institutional Animal Care and Use Committee and the US Army Medical Research and Materiel Command Animal Care and Use Review Office.

Animals were induced using subcutaneously administered ketamine hydrochloride (20–40 mg/kg) and xylazine (3–5 mg/kg). Given the unique metabolic rate of each rabbit, subcutaneous induction resulted in a variable duration of sedation during each procedure. As a result, rabbits were intubated and maintained on isoflurane gas (2%–4%), which was titrated to effect. The chest and base of the ears were prepared for the procedure by removal of hair with an electric razor and then sterilized with betadine and alcohol (Fig. 2).

Costal Cartilage Harvest

A 3-cm incision was made lateral to the sternoxyphoid junction through the external oblique muscle. The sixth rib, containing a large amount of bulk tissue, was identified, and 25 mm of costal cartilage was harvested.[16] The incision was then closed and an identical procedure was performed on the contralateral hemithorax.

Electromechanical Reshaping

The harvested costal tissue was then carefully stripped of perichondrium and carved into a 1.0 mm × 2.5 mm × 25 mm segment. Each prepared rib was then placed in a custom ceramic jig that approximated the contour of the auricular base of the rabbit pinna, as developed in previous work.[17] Four needle electrodes spaced 3 mm apart were inserted along the greatest curvature of the mold allowing for charge transfer. The voltage and time settings investigated are summarized in Table I and are derived from ex vivo experiments.[9,17,18] Control specimens underwent the same procedure without the transfer of current.

Defect and Implantation

A 4-cm incision was made along the base of the ear skin at the anterior curvature, exposing the auricular cartilage. A 25 × 3-mm rectangular segment of auricular cartilage was resected while maintaining the integrity of the underlying perichondrium. The reshaped costal cartilage graft was then inserted into the surgically created defect at the auricular base, and a figure of eight suture was placed to maintain the position of the graft. Overlying skin flaps were then closed, and the same procedure was performed on the opposite ear. A bolster made of Xeroform dressing (Covidien, Mansfield, MA) was sutured to the auricular base to minimize the risk of auricular hematoma around the graft. Following surgery, the animals were observed and examined daily for signs of pain, infection, and other operative complications. Tissue bolster was removed 5 days after the procedure.

Analysis of Shape Change

All costal cartilage specimens were photographed prior to and following EMR. The degree of shape change was determined using digital micrometry as previously described.[19] First, the convex surface of the cartilage was segmented in Photoshop CS6 (Adobe Systems, Inc. San Jose, CA). This curve arc segment was then imported into Engauge Digitizer 4.1 (freeware, Mark Mitchell, http://digitizer.sourceforge.net), which generated points along the contour and tabulated the data as x-y coordinates. SigmaPlot 11 (Systat Software Inc., San Jose, CA) then used the tabular data to create a scatter plot. Regression analysis was then used to fit a quadratic function, of the form $y = ax^2 + bx + c$, to the curve. The coefficient a describes the width of the fitted parabola, and thus the amount of bend. Increased curvature of a specimen yields a higher value of the coefficient a. Student t test was used to compare shape change among specimens.

Cellular Viability Analysis

Following euthanasia, the graft implant site was dissected, and a 13-mm segment of costal cartilage was collected. The resected tissue was bifurcated lengthwise and stained for 30 minutes using the LIVE/DEAD assay (Invitrogen, Eugene, OR) as described in previous studies.[15,20] To visualize the distribution of live and dead cells, cross-sectional imaging was performed using a laser scanning confocal microscope (LSM 510 META; Carl Zeiss, Jena, Germany). The extent of chondrocyte injury at the site of needle insertion was measured between islands of viable cells.

Semiquantiative Histologic Analysis

The remaining implanted segment of costal cartilage graft and adjacent auricular base tissue was formalin fixed, paraffin embedded, and stained with hematoxylin and eosin (H&E) stain. One scientist blinded from the study and experienced in cartilage histology qualitatively rated cartilage degeneration, tissue structure, and fibrosis on a four-point Likert scale. A score of 1 categorized specimens that were closest to normal unaltered costal cartilage. A score of 4 represented specimens with severe disruption of native tissue architecture that extended through the entire width of the graft. Such deviations included the formation of fibrous tissue, extracellular matrix loss, empty lacunae, as well as loss of smooth surface architecture with no obvious collagen fiber organization. Scores of 2 or 3 represented mild or moderate deviations including partial thickness matrix damage, the presence of few inflammatory cells, and surface disruption with collagen fibers intact. Statistical analysis of the results was performed using one-way general linear model analysis of variance to determine if the means tabulated from the experimental and control groups were different among survival durations. Also, any evidence of neochondrogenesis was noted.

RESULTS

Twenty-five of 31 New Zealand white rabbits were studied following a 6- or 12-week survival duration. Intraoperative mortalities included pneumothorax (n = 4 rabbits) and endotracheal tube dysfunction (n = 2 rabbits). Of the 50 successful costal cartilage auricular

implants, tissue morbidity caused by graft ischemia (n = 4 ears) and tissue necrosis during histological processing (n = 6 ears) resulted in the analysis of 40 implanted ears.

On visual examination following euthanasia, all operative sites appeared similar to the preoperative auricular base without any skin or soft tissue lesions. The incision and implantation sites appeared well healed.

Shape Change and Gross Findings

Average bend angle increased with increasing voltage and charge transfer. The amount of bend increased from a coefficient of $5.0 \times 10^{-4} \pm 1.0 \times 10^{-4}$ in control specimens to $3.0 \times 10^{-3} \pm 1.0 \times 10^{-3}$ in the 6 V 3 min–treated cartilage, which was statistically significant ($P <$ .01). In control specimens, when comparing pre- and post-treatment bend angles, there was no significant difference in shape change ($P = .40$). Figure 3 illustrates the shape change prior to and following EMR in control and experimental specimens. Figure 4 provides a summary of the bend angle coefficients for all conditions.

A circular translucent region of 1 mm to 3 mm in diameter was observed at the needle insertion sites of treated specimens that grew in diameter with increasing voltage. All experimental specimens demonstrated shape fidelity to the contour of the auricular base on gross examination. Control specimens, however, did not conform to the curvature of the auricular base. In fact, control specimens at harvest were straighter and deviated from the natural curvature of the auricular base. This protrusion at both ends of the graft raised the overlying skin/soft tissue. Figure 5 provides both gross and histologic evidence of this protrusion deformity. All costal grafts, both control and experimental, were brittle and had some mineralization.

Cellular Viability

Control specimens using confocal microscopy with the LIVE/DEAD assay demonstrated live green chondrocytes uniformly distributed throughout the tissue matrix. All experimental EMR specimens produced small focal areas of cell death and extracellular matrix devoid of viable chondrocytes (Fig. 6). These areas of nonviable cells were identified by a pervasive “red” signal that extended away (range, 2.0–3.9 mm) from the point of needle electrode insertion sites, sharply flanked by living “green” chondrocytes. Figure 7 demonstrates the progressive tissue injury with increasing application of voltage and survival duration. In control specimens, no gross tissue injury was observed.

Histologic Analysis

H&E staining identified focal cartilage injury at the electrode insertion sites of experimental specimens. In treated specimens where electrodes were placed, empty lacunae with differential matrix staining were identified (Fig. 8). The diameter of injury, although modest, increased with greater application of voltage (range, 2–3 mm) and was in agreement with LIVE/DEAD assay measurements above.

Semiquantitative and Histologic Analysis

Experimental specimens differed from control samples at both 6 and 12 weeks. Extracellular matrix loss resembling tissue degeneration was more prevalent and severe in EMR-treated tissues at 12 weeks when compared to control samples ($P = .023$). Likewise, the formation of fibrous tissue was uniquely a feature of 12-week experimental specimens ($P = .049$). Six-week control specimens largely maintained their smooth tissue architecture, unlike experimental specimens, at needle insertion sites ($P = .024$). The difference in surface structure at 12 weeks, however, was insignificant ($P = .47$). New cartilage formation was also identified adjacent to and within needle sites in 88% (n = 16 of 18) of 6-week specimens and 62% (n = 13 of 21) of 12-week specimens.

DISCUSSION

Auricular reconstruction is a technically challenging procedure that utilizes a limited supply of costal cartilage. Even with advanced sectioning techniques, shape change of this relatively brittle tissue still remains a challenge, and suture techniques alone may be inadequate. The present work focuses upon evaluating the use of EMR technology to reshape costal cartilage in this preclinical surgical model, as EMR treatment of costal cartilage grafts has not been previously studied in vivo.

Our study demonstrates that spatially localized tissue injury and cell death is part of the tradeoff required to establish new shape equilibrium. We have also observed that a time-voltage parameter exists where shape change and adequate chondrocyte viability are achieved. Cell and tissue injury is on par with that encountered during common procedures such as morselization, albeit with EMR the injury is highly localized.[21] By carefully identifying key regions of increased internal stress, EMR may potentially be applied in a spatially selective manner to achieve adequate shape change without significant compromise in tissue viability.

Our surgical technique was modified throughout the study to reduce rabbit morbidity and mortality. Prior to this study, in vivo surgical models for microtia have not been reported, and a significant learning curve was encountered. Pneumothorax proved to be the most frequent cause of intraoperative mortality (n = 4 rabbits). Although this is an anticipated complication when dissecting cartilage along the posterior perichondrium in a medium-sized animal, we modified our technique and utilized cotton swabs for blunt dissection rather than cold knife sharp dissection in harvesting tissue. Also, malpositioned endotracheal tubes resulted in airway compromise and mortalities (n = 2 rabbits), and this reflects our learning curve with this model. Graft ischemia and necrosis led to the postoperative morbidity of four ears due to bolstering techniques. Also, six specimens were regrettably lost during histological processing.

Significant shape change with contouring to the auricular base was achieved and retained following EMR. Again, we noted greater shape change with greater charge transferred. Our understanding is that it is the total charge transferred, and not the specific voltage or time application, that guides the degree of reshaping.[22] To that end, there are several factors that modify the amount of charge transferred that would necessitate recording the charge

delivered while undergoing EMR. Factors that affect charge transfer include specimen thickness and water content. Additionally, although greater charge resulted in greater shape change, it is likely that this relationship to shape change will eventually diminish above a certain dosimetry as the cartilage matrix is modified by electrochemical reactions.

As cartilage is an avascular tissue that undergoes a cascade of events when injured, including chondrocyte depopulation, depletion of proteoglycans, calcification, fibrosis, and chondroblast repopulation, assessing tissue repair in vivo is necessary when observing the effects following cartilage reshaping.[11,23] Histology identified depletion of normal extracellular matrix and differential tissue staining pattern at the needle insertion sites in all treated specimens. The areas of injury were surrounded longitudinally by abundant normal-appearing native costal cartilage, contributing to an adequate integrated response to thumb and forefinger flexure. Twelve-week specimens were qualitatively more resistant to this deformation and demonstrated greater elasticity, which is consistent with the observed difference in fibrosis between the two survival groups ($P = .02$). The difference in overall structure among 6-week specimens reflects the acute effect of EMR on needle insertion sites in treated specimens. Over time, however, experimental and control surface structures did not differ, demonstrating the long-term effects of an in vivo system on tissue implants. New cartilage formation was also observed in experimental and control specimens within the native auricular tissue and in the costal cartilage needle insertion sites. Chondroblasts have been observed to migrate into regions of injured cartilage from adjacent areas in osteoporosis studies.[24–26] It is important to note, however, that the chondrogenic response in our study may have been augmented by the native auricular perichondrium found within the graft site. The perichondrium was left in place to maintain the retention forces at the base of the auricle to better support the graft pocket.

Chondrocyte viability utilizing laser confocal microscopy with the LIVE/DEAD fluorescent assay revealed increased cell death with increasing potential difference, similar to the outcome of previous ex vivo studies.[15,17] This is also confirmed by our semiquantitative analysis (Table II), where degeneration increased with increasing voltage-time parameters. Concentrated areas of tissue injury were limited to the immediate vicinity around each needle electrode with a maximum diameter of 3.9 mm at 6 V. Areas of chondrocyte necrosis or apoptosis, unlike ex vivo or short-term in vivo studies, were characterized by a space devoid of cellular matter, suggesting an active phagocytic inflammatory process, within the living system.[11,15,17] Overall, the degree of tissue injury is limited in spatial extent, allowing for shape change with only localized cell injury.

The objective herein was to investigate the dosimetry effect of EMR in costal cartilage in an in vivo long-term animal model, examine cartilage shape change stability, determine the tissue cellular response, and develop expertise with the rabbit costal cartilage surgical model. Our study has demonstrated that EMR alters and maintains the shape of tissue with only focal sites of cell death and a localized cellular response. Although we have begun to demonstrate the varying tissue changes that can occur with this technology, further investigation is needed to evaluate the response to a broader range of voltage-time parameters and even longer implantation intervals. Moreover, specific characterization of the pH gradient occurring at anode and cathode sites will enhance our understanding of the

tissue changes occurring within the cartilaginous matrix.[27] Finally, the mechanical behavior of reshaped tissue can be further assessed via detailed mechanical analysis and finite element modeling to quantitatively assess the response to physical deformation following EMR.

CONCLUSION

EMR is a viable technique to create shape change in vivo in the costal cartilage–auricular base rabbit model. This technology relies on creating focal regions of change in tissue mechanical properties with only modest and spatially limited cell and tissue injury. Optimizing the preservation of chondrocytes with clinically relevant shape change warrants further in vivo studies. Future studies to assess the response to injury with longer durations of survival, greater variations in dosimetry, and an advanced characterization of mechanical and electrochemical behavior will be required before clinical application.

Acknowledgments

This work was supported by the Department of Defense Deployment Related Medical Research Program (DR090349), Air Force Office of Scientific Research (FA9550–04–1–0101), the National Institutes of Health (DE019026, DC005572, DC 00170, RR 01192), and the Lockheed Martin Corporation (LMC-46674).

BIBLIOGRAPHY

1. Tanzer RC. Total reconstruction of the external ear. Plast Reconstr Surg Transplant Bull. 1959; 23:1–15. [PubMed: 13633474]
2. Brent B. The correction of mi-rotia with autogenous cartilage grafts: I. The classic deformity Plast Reconstr Surg. 1980; 66:1–12. [PubMed: 7394028]
3. Firmin F. Ear reconstruction in cases of typical microtia. Personal experience based on 352 microtic ear corrections. Scand J Plast Reconstr Surg Hand Surg. 1998; 32:35–47. [PubMed: 9556819]
4. Nagata S. A new method of total reconstruction of the auricle for microtia. Plast Reconstr Surg. 1993; 92:187–201. [PubMed: 8337267]
5. Sforza C, Grandi G, Binelli M, Tommasi DG, Rosati R, Ferrario VF. Age-and sex-related changes in the normal human ear. Forensic Sci Int. 2009; 187:110.e1–7. [PubMed: 19356871]
6. Foulad A, Hamamoto A, Manuel C, Wong BJ. Precise and rapid costal cartilage graft sectioning using a novel device: clinical application. JAMA Facial Plast Surg. 2013; 16:107–112. [PubMed: 24337405]
7. Gandy, JT.; Manuel, CT.; Nguyen, T.; Wong, BJ. The future of auricular repair: using EMR to develop a minimally invasive technique to build a human ear. Military Health System Research Symposium; Fort Lauderdale, FL. August 18–21, 2014;
8. Ho K-HK, Diaz Valdes SH, Protsenko DE, Aguilar G, Wong BJF. Electromechanical reshaping of septal cartilage. Laryngoscope. 2003; 113:1916–1921. [PubMed: 14603047]
9. Manuel CT, Foulad A, Protsenko DE, Hamamoto A, Wong BJ. Electromechanical reshaping of costal cartilage grafts: a new surgical treatment modality. Laryngoscope. 2011; 121:1839–1842. [PubMed: 22024834]
10. Wu EC, Protsenko DE, Khan AZ, Dubin S, Karimi K, Wong BJF. Needle electrode-based electromechanical reshaping of rabbit septal cartilage: a systematic evaluation. IEEE Trans Biomed Eng. 2011; 58(8)
11. Karamzadeh AM, Chang JC, Diaz S, Milner ET, Wong BJF. Long-term in vivo stability of rabbit nasal septal cartilage following laser cartilage reshaping: a pilot investigation. Lasers Surg Med. 2005; 36:147–154. [PubMed: 15704163]
12. Ovchinnikov Y, Sobol E, Svistushkin V, Shekhter A, Bagratashvili V, Sviridov A. Laser septochondrocorrection. Arch Facial Plast Surg. 2002; 4(3):180–185. [PubMed: 12167077]

13. Bagratashvili VN, Sobol EN, Sviridov AP, Popov VK, Omel'chenko AI, Howdle SM. Thermal and diffusion processes in laser-induced stress relaxation and reshaping of cartilage. J Biomech. 1997; 30:813–817. [PubMed: 9239566]
14. Karam AM, Protsenko DE, Li C, et al. Long-term viability and mechanical behavior following laser cartilage reshaping. Arch Facial Plast Surg. 2006; 8:105–116. [PubMed: 16549737]
15. Oliaei S, Manuel C, Karam B, et al. In vivo electromechanical reshaping of ear cartilage in a rabbit model: a minimally invasive approach for otoplasty. JAMA Facial Plast Surg. 2013; 15:34–38. [PubMed: 23117484]
16. Badran KW, Waki C, Hamamoto A, Manz R, Wong BJF. The rabbit costal cartilage reconstructive surgical model. Facial Plast Surg. 2014; 30:76–80. [PubMed: 24488642]
17. Badran K, Manuel C, Waki C, Protsenko D, Wong BJF. Ex vivo electromechanical reshaping of costal cartilage in the New Zealand white rabbit model. Laryngoscope. 2013; 123:1143–1148. [PubMed: 23553270]
18. Manuel CT, Foulad A, Protsenko DE, Sepehr A, Wong BJF. Needle electrode-based electromechanical reshaping of cartilage. Ann Biomed Eng. 2010; 38:3389–3397. [PubMed: 20614240]
19. Foulad, A.; Manuel, C.; Kim, J.; Wong, BJF. Numerical analysis of costal cartilage warping after laser modification. In: Kollias, N.; Choi, B.; Zeng, H., et al., editors. Photonics Therapeutics and Diagnostics VI. Bellingham, WA: International Society for Optics and Photonics; 2010. p. 75482M-75482M-6.
20. Chae Y, Protsenko D, Holden PK, Chlebicki C, Wong BJF. Thermoforming of tracheal cartilage: viability, shape change, and mechanical behavior. Lasers Surg Med. 2008; 40(8):550–561. [PubMed: 18798288]
21. Protsenko DE, Ho K, Wong BJF. Survival of chondrocytes in rabbit septal cartilage after electromechanical reshaping. Ann Biomed Eng. 2011; 39:66–74. [PubMed: 20842431]
22. Protsenko DE, Ho K, Wong BJF. Stress relaxation in porcine septal cartilage during electromechanical reshaping: mechanical and electrical responses. Ann Biomed Eng. 2006; 34:455–464. [PubMed: 16450186]
23. Mordon S, Wang T, Fleurisse L, Creusy C. Laser cartilage reshaping in an in vivo rabbit model using a 1. 54 microm Er:Glass laser. Lasers Surg Med. 2004; 34:315–322. [PubMed: 15083492]
24. Seol D, McCabe DJ, Choe H, et al. Chondrogenic progenitor cells respond to cartilage injury. Arthritis Rheum. 2012; 64:3626–3637. [PubMed: 22777600]
25. Grogan SP, Miyaki S, Asahara H, D'Lima DD, Lotz MK. Mesenchymal progenitor cell markers in human articular cartilage: normal distribution and changes in osteoarthritis. Arthritis Res Ther. 2009; 11:R85. [PubMed: 19500336]
26. Otsuki S, Grogan SP, Miyaki S, Kinoshita M, Asahara H, Lotz MK. Tissue neogenesis and STRO-1 expression in immature and mature articular cartilage. J Orthop Res. 2010; 28:96–102. [PubMed: 19603515]
27. Kuan EC, Hamamoto AA, Manuel CT, Protsenko DE, Wong BJF. In-depth analysis of pH-dependent mechanisms of electromechanical reshaping of rabbit nasal septal cartilage. Laryngoscope. 2014; 124:E405–E410. [PubMed: 24687330]

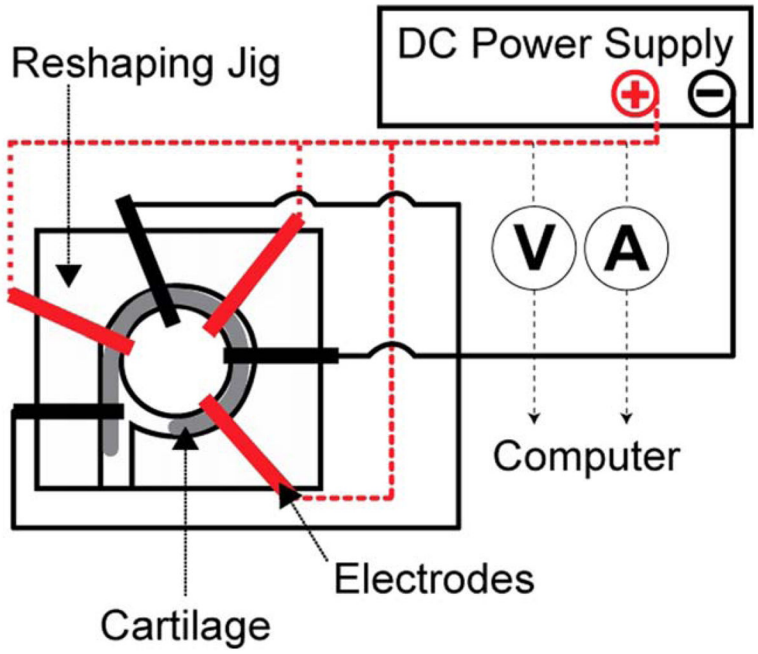

Fig. 1.

Electromechanical reshaping schematic. DC = direct current; V = voltage; A = ampere. [Color figure can be viewed in the online issue, which is available at www.laryngoscope.com.]

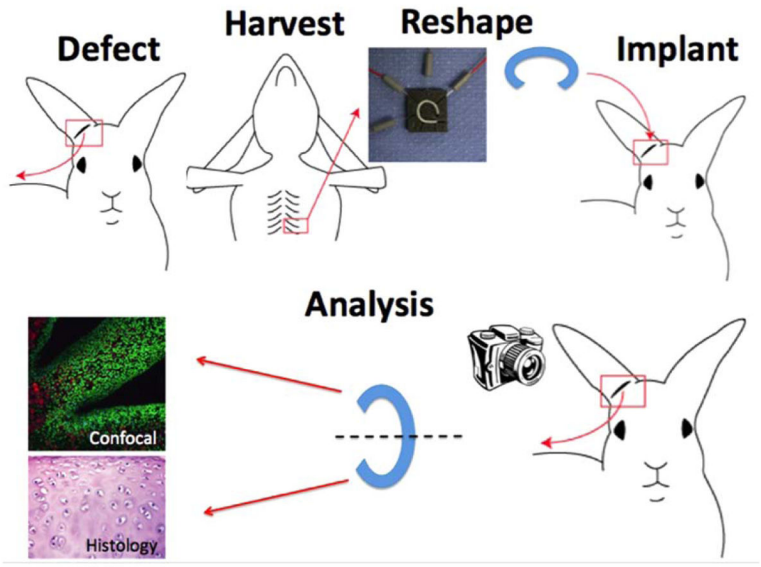

Fig. 2.

A costal cartilage graft is harvested while a defect is created in the cartilaginous framework of the auricular base. The costal graft then undergoes electromechanical reshaping and is implanted in the auricular defect for either 6 or 12 weeks. Following euthanasia, the base of the ear is analyzed with digital photography, confocal microscopy, and histology. [Color figure can be viewed in the online issue, which is available at www.laryngoscope.com.].

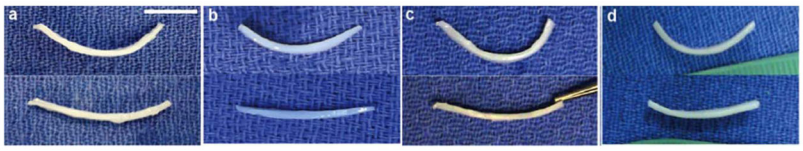

Fig. 3.

Costal cartilage segments pre–electromechanical reshaping (below) and following treatment (above). From left to right: (a) control, (b) 4V 3min, (c) 5V 3min, and (d) 6V 3min. [Color figure can be viewed in the online issue, which is available at www.laryngoscope.com.].

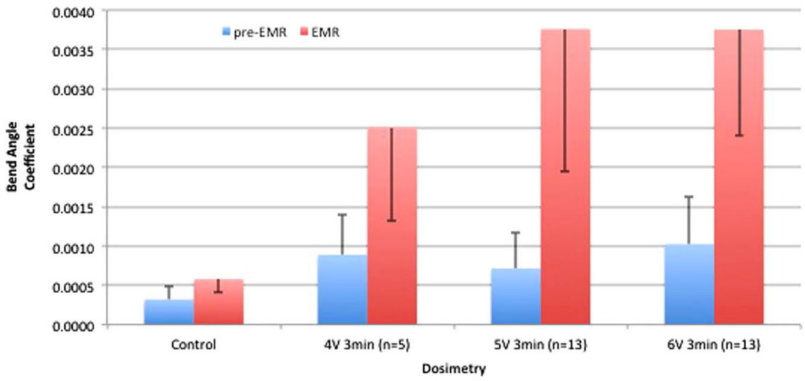

Fig. 4.

This graph illustrates the mean degree of shape change ± standard error with voltage-time parameters. EMR = electromechanical reshaping. [Color figure can be viewed in the online issue, which is available at www.laryngoscope.com.].

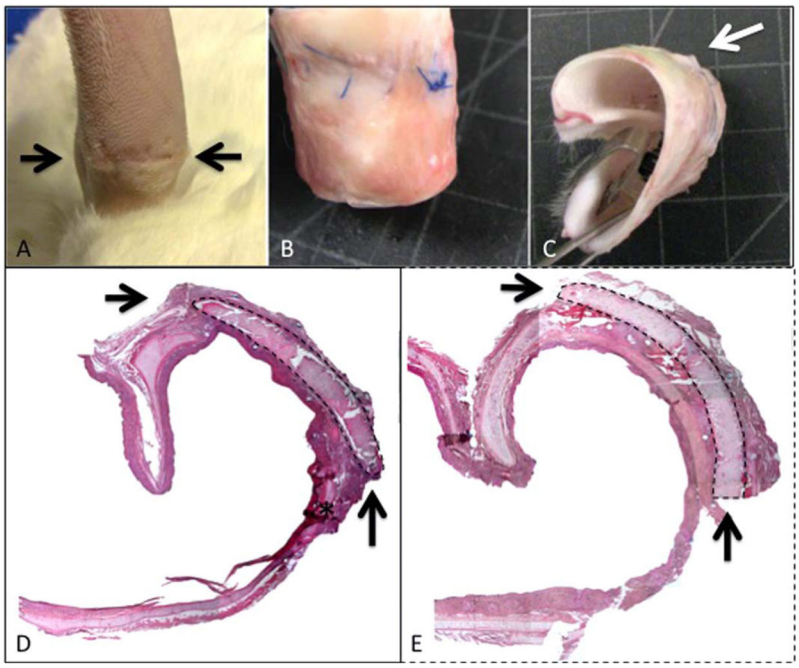

Fig. 5.

(A–C) The rabbit auricular base at 6 weeks with control costal cartilage graft in place. (A) Auricular skin intact with arrows denoting implant site. (B) Skin dissected with sutures in place. (C) Axial view of the auricular base with arrow illustrating the terminal end of the costal cartilage implant. (D) Histologic view (1×, hematoxylin and eosin) of control specimen at 6 weeks. The arrows denote terminal ends of costal cartilage implant, and the dashed line outlines costal graft. The implant does not contour to the auricular base. Asterisks (*) denote fibrous tissue filling in space between auricular base and cartilage graft. (E) View of 4V 3min electromechanical reshaping–treated specimen. Arrows denote terminal ends of implant. The implant adequately contours to the base of the auricle. [Color figure can be viewed in the online issue, which is available at www.laryngoscope.com.].

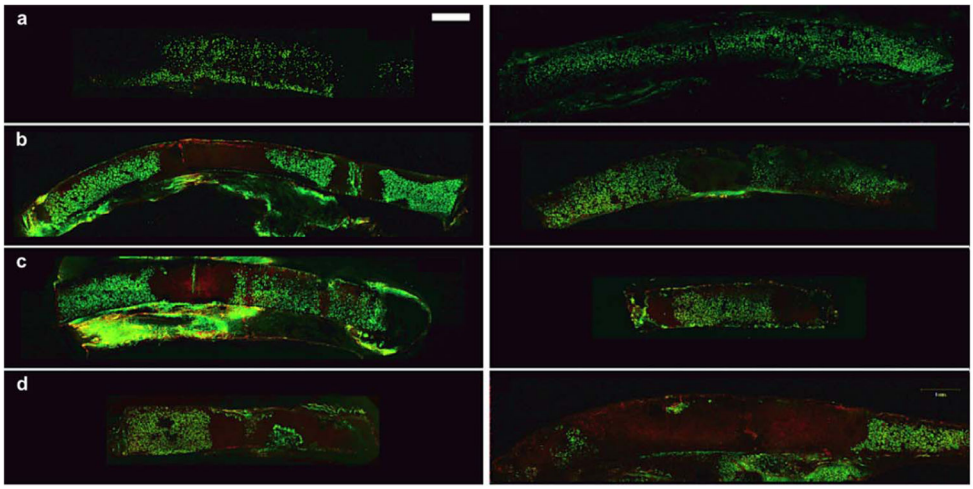

Fig. 6.

Confocal microscopy and viability assay at 6 and 12 weeks following electromechanical reshaping. Green represents living and red represents dead chondrocytes. (a–d) Results at 6 and 12 weeks (left and right, respectively), with increasing dosimetry from top to bottom, (a) control, (b) 4V, (c) 5V, and (d) 6V. [Color figure can be viewed in the online issue, which is available at www.laryngoscope.com.].

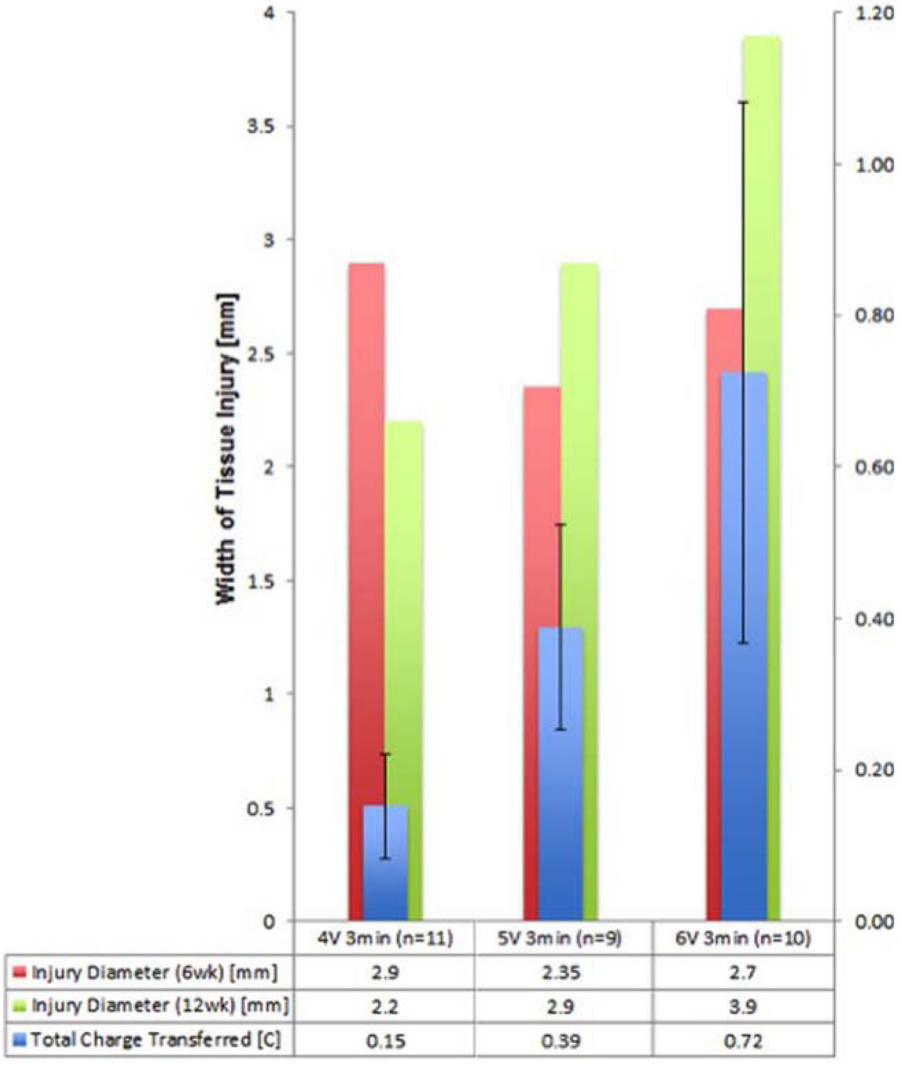

Fig. 7.

Tissue injury and charge transferred. Represents the median value of tissue injury identified in LIVE/DEAD assay and average charge transferred ± standard error, among the increasing voltage-time parameters. [Color figure can be viewed in the online issue, which is available at www.laryngoscope.com.].

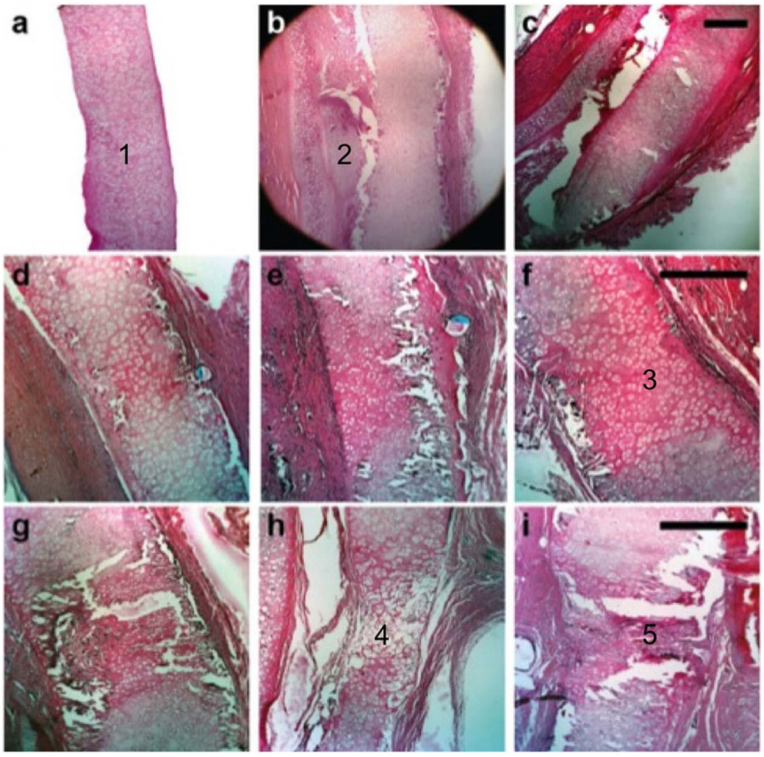

Fig. 8.

Histology. First row illustrates control specimens: (a) Preimplantation costal cartilage with (1) normal extracellular matrix and abundant chondrocytes. (b) Specimen at 6 weeks survival and (2) island of chondrogenesis. (c) Specimen at 12 weeks survival. Second row depicts 6-week experimental specimens: (d) 4V 3min, (e) 5V 3min (f) 6V 3min. Differential matrix staining pattern and empty lacunae (3) demonstrate tissue matrix injury. Third row illustrates 12-week experimental specimens: (g–i) 4V–6V. Sectioning artifact (4) resembles weakened native tissue; fibrocartilage is also present (5). [Color figure can be viewed in the online issue, which is available at www.laryngoscope.com.].

TABLE I

Summary of Investigated EMR Parameters.

EMR Parameter Set	Survival Duration, wk	Costal Cartilage Group Size
4V 3min	6	6
4V 3min	12	6
5V 3min	6	5
5V 3min	12	7
6V 3min	6	5
6V 3min	12	7
Control	6	2
Control	12	2

EMR = electromechanical reshaping.

TABLE II

Histologic Semiquantitative Analysis.

		Chondrogenesis	Degeneration	Fibrosis	Surface Structure
Control	6 wk	3 of 3	1.67	1	1.67
	12 wk	1 of 2	1	1	3.5
4V 3min	6 wk	4 of 4	2	1	2.25
	12 wk	5 of 7	3.14	3	2.57
5V 3min	6 wk	5 of 5	2.4	1.8	3
	12 wk	3 of 6	2.83	2.67	3
6V 3min	6 wk	4 of 6	3.2	1.6	3
	12 wk	4 of 6	4	3.17	3.17
ANOVA 6 wk			*P* = .100	*P* = .091	*P* = .024
ANOVA 12 wk			*P* = .023	*P* = .049	*P* = .471

ANOVA = analysis of variance.